

Montmorillonite clay intercalated with nanoparticles for hydrogen storage

Fabiola Campos^a, Luis de la Torre^a, Manuel Román^a, A. García^b and A. Aguilar Elguézabal^{a,*}

^aCentro de Investigación en Materiales Avanzados (CIMAV), Miguel de Cervantes No. 120, Chihuahua, C.P. 31109, México

^bInterceramic, R & D Dept., Av. Carlos Pacheco #7200 Chihuahua, 31060, México

According to the expectations around the world concerning future of energy sources, hydrogen will be in a few years the most important energy carrier for stationary and mobile applications. Hydrogen storage is the bottleneck on the race to commercialize technologies based on the use of hydrogen, and specifically for mobile applications, the research goal for 2010 is to develop a device with at least 6% w/w of storage capacity. Highly porous carbon-based materials are among the most promising materials, with Carbon Molecular Sieves (CMS) and Carbon Nanotubes (CNT) the most studied. In both cases materials are structured in such a way that hydrogen must diffuse along channels (micropores) where walls represent a restriction for the adsorption/desorption cycle. In this study, an alternative material is prepared by separation of clay layers with silica nanoparticles of diameter around 12 nm. The hydrogen storage capacity increased from 0.12 for untreated clay to 0.40% w/w for nanoassembled clay, measured at 77 K and atmospheric pressure, and according to intercalated clay characterization, almost all the surface available on the clay was exposed for adsorption.

Key words: Hydrogen storage, Montmorillonite, Clay, Nano-assemblies.

Introduction

Global warming (mainly due to CO₂ emission) and price rises of hydrocarbon-based fuels are problems that motivate the search for alternative sources of energy [1, 2]. In this context, the use of hydrogen becomes an attractive choice, especially for hydrogen produced by water electrolysis, which is environmentally friendly. Technologies to use hydrogen as an energy source are already commercially available with adequate performance; nevertheless, the storage of hydrogen is the bottleneck that limits the commercial boom in these technologies, since an economic, safe and light weight system is required [3].

Among the options that are currently under study for hydrogen storage, the use of porous materials seems to have high potential, since a range of temperatures can be used, and pressure may be significantly lower than required for storage as compressed gas [4]. However, for Carbon based Molecular Sieves (CMS) [5] and Carbon Nanotubes (CNT) [6], which are the most studied materials, hydrogen storage requires the diffusion through tubular-type pores where the access is mainly from only one side. For this reason, accessibility to the whole available surface is from the point-of-view of energy, low and thus favorable and adsorption/desorption kinetics may be affected.

To minimize diffusion problems, a structure of thin sheets separated by pillars would be ideal, considering that

then the accessibility to available surface is not restricted to one dimension. Clays are naturally layer-structured materials, and as was clarified in a previous study [7], if both sides of each layer are accessible to N₂ molecules during surface area measurements, then the surface area could be higher than 750 m² g⁻¹. Kawi reported [8] a method to obtain an intercalated structure in which single layers of clay were separated and SiO₂ particles of silica were used to keep the layers separated. According to our experience the structure was unstable and easily collapsed, thus losing the accessibility to the spatial separation of clay layers. In this study we report a method to obtain an intercalated clay, structured by almost single clay layers separated by SiO₂ nanoparticles which are pretreated to obtain a stable array with the highest surface area possible. This nanostructured array is used as a base to develop a hydrogen storage material.

Experimental

The method to assemble the expanded and intercalated clay was previously reported by Kawi [8] and to improve the stability of the expanded structure of the intercalated clay, silica particles were previously treated to hydroxylate their surfaces. One gram of clay (untreated montmorillonite clay from Fluka, with 128 m² g⁻¹ of surface area) was suspended in 5 ml of water and maintained in suspension overnight, thus the clay swelled. An aqueous solution of cetyltrimethylammonium hydroxide (CTMAOH) was prepared by the ion exchange of cetyltrimethylammonium bromide (CTMABr, from Sigma) with Amberlite IRA-400-OH resin (from Rohm & Haas). The CTMAOH

*Corresponding author:
Tel : +52-614 439 1109
Fax: +52-614 439 1130
E-mail: alfredo.aguilar@cimav.edu.mx

solution was concentrated to 16.8% w/w. To promote the formation of hydroxyl groups on the surface of silica particles (Aerosil-200 from Degussa, $200 \text{ m}^2 \text{ g}^{-1}$), 0.4 g of SiO_2 particles were suspended in water under stirring and heating and maintained overnight under reflux. 20 g of CTMAOH solution, swelled clay and silica were mixed and maintained under stirring for 5 h, afterwards the suspension was transferred to an autoclave. The hydrothermal treatment was maintained for 48 h at 96°C . The autoclave was open and maintained at the same temperature for drying for 12 h. Calcining was done at 550°C for 2 h, and the heating rate was 1 K minute^{-1} .

To evaluate the textural parameters of the samples, physical adsorption of N_2 at 77 K was carried out in an automatic gas sorption analyzer (Quantachrome Autosorb 1c). Prior to the measurements, the samples were outgassed at 300°C for 3 h. Surface areas (BET area) were obtained using the multipoint BET method. A Quantachrome Autosorb 1c apparatus was used to measure the hydrogen adsorption isotherms at 77 K from 0.05 to $0.995P/P_0$. The isotherm consists of 20 points of adsorption and 20 points of desorption. P_0 represents the atmospheric pressure, 660 mmHg for Chihuahua City. The hydrogen adsorption capacity was determined using the value of the adsorbed volume at $0.995P/P_0$ and the ideal gas equation. The value of $0.995P/P_0$ is very close to the value of the atmospheric pressure. High purity hydrogen was used in this study. X-Ray diffraction (XRD) was made on a Phillips XPert MPD diffractometer using monochromatized $\text{CuK}\alpha$ radiation. Microscopic examinations were made on a TEM (Phillips CM200), powder samples were dispersed in ethyl alcohol, sonicated in an ultrasonic cleaner for 5 minutes and a drop was deposited on to a 3 mm diameter copper grid.

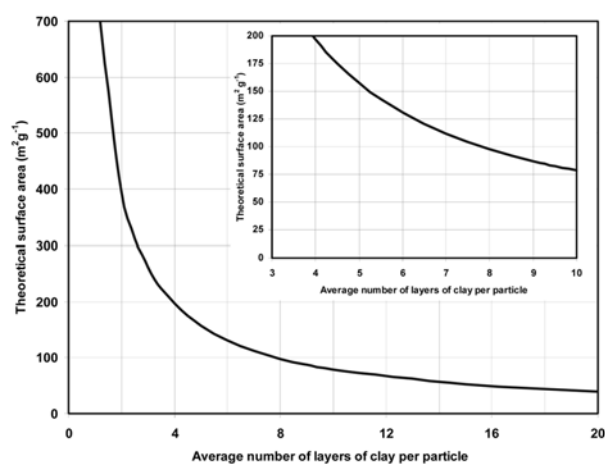


Fig. 1. Theoretical surface area of montmorillonite clay as a function of the average number of clay layers that comprise a particle, considering that all particles have the same number of clay layers, as reported in [7].

Results and Discussions

Natural montmorillonite clay used in this study has $128 \text{ m}^2 \text{ g}^{-1}$ surface area, thus according to our previous study [7], clay is arranged as elementary particles that are composed by around six aluminosilicate layers and N_2 does not have accessibility to the interlayer surface, so the BET surface area corresponds to the sum of the external surface areas of each block of six layers (see Fig. 1). Under this concept, there are two ways to increase the surface area: to reduce the number of clay layers per particle or to separate clay layers at such a distance that nitrogen molecules could have access to the interlaminar surface. By the process of intercalation of nanoparticles described here, a mixture of both processes can be obtained, since

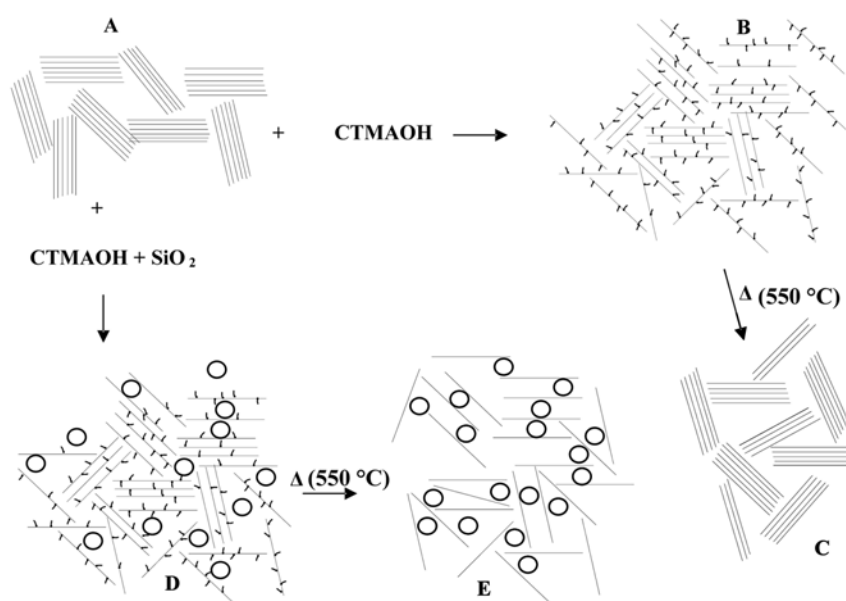


Fig. 2. Schematic representation of the structure of natural clay (A); clay after hydrothermal treatment using only CTMAOH (B) and after calcination (C); clay after hydrothermal treatment using CTMAOH and SiO_2 nanoparticles and after calcination (D and E).

the function of surfactant CTMAOH is to increase the interlayer separation, at least as required to let the SiO_2 nanoparticles enter into the space created by the separation of the clay layers and during calcining, the burning of the surfactant leads to a disordered structure where silica nanoparticles obstruct the compaction of layers to restore the original structure. Probably some clay layers are stacked with a typical separation given by the diameter of the nanoparticles, and some layers remain as unaligned single clay layers as shown in Fig. 2. Under the absence of silica nanoparticles clay layers tend to collapse like if they were at the beginning of process and only a small increase of surface area is obtained (from 128 to $190 \text{ m}^2 \text{ g}^{-1}$), indicating that the average number of clay layers per particle has slightly decreased (represented as “C” in Fig. 2).

According to the synthesis method described, the composition of intercalated clay was 71% clay and 29% SiO_2 . After several syntheses, the mean surface area of intercalated clay was $590 \pm 27 \text{ m}^2 \text{ g}^{-1}$. For all cases the value was higher than the simple addition of the surface area of each component, i.e. $148 \text{ m}^2 \text{ g}^{-1}$ ($200 \times 0.29 + 128 \times 0.71$), which supports the idea that after calcination, the structure is similar to the represented in Fig. 2 (E). Isotherms of nitrogen adsorption are shown in Fig. 3. As can be seen, for both treated clays the mesoporosity increases, but adsorption at low P/Po values clearly shows that there is higher surface available for N_2 adsorption for the clay intercalated with SiO_2 nanoparticles. According to the XRD (Fig. 4) spectra of natural clay, the separation from clay layer to clay layer is 1.58 nm (from Bragg's Law) and considering that thickness of a clay layer is 0.98 nm , then the separation between clay layers is around 0.5 nm , theoretically this distance is enough for N_2 diffusion in the interlayer space, but the presence of cations and interlaminar water restrict the access and thus the surface area measured by N_2 adsorption is only due to the external surfaces of particles. As can be seen from the XRD pattern of

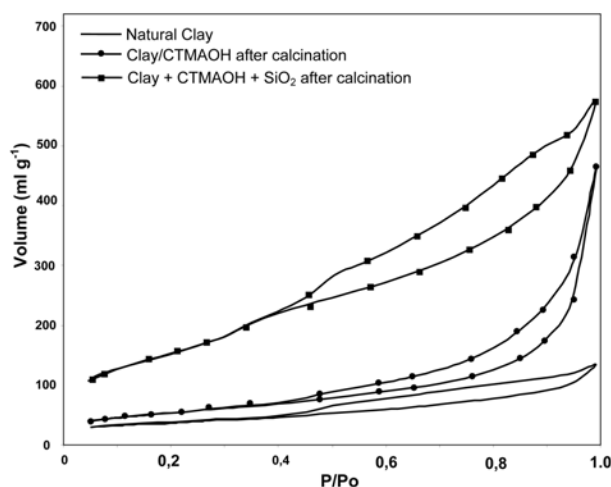


Fig. 3. Nitrogen adsorption isotherms of natural clay and clay hydrothermally treated with CTMAOH and calcined and hydrothermally treated with CTMAOH and SiO_2 and calcined.

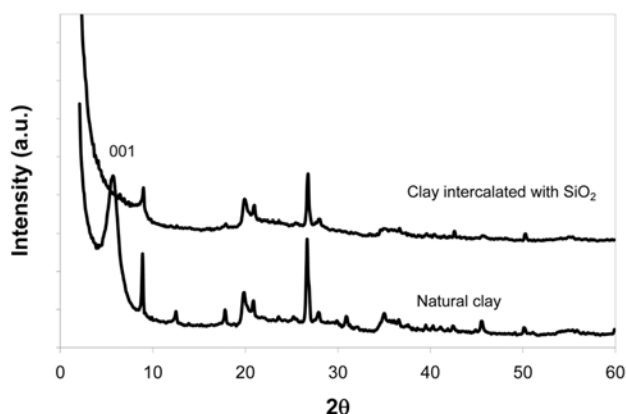


Fig. 4. XRD of natural and intercalated clay.

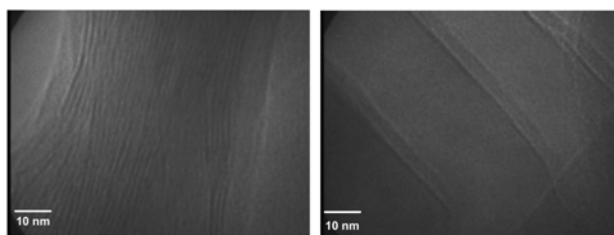


Fig. 5. TEM images of the natural clay before treatment (left) and after the insertion of SiO_2 nanoparticles (right).

intercalated clay, the 001 signal disappears, so the stacking of layers vanishes or the distance between the layers increases beyond the detection limit of the diffractometer, probably due to the formation of an arrangement as depicted on Fig. 2 E. Fig. 5 shows the images obtained by transmission electron microscopy (TEM), and as can be seen, untreated clay consists of stacked clay layers, and after the insertion of SiO_2 nanoparticles, the structure changed and bilayers of clay are separated from each other by around 12 nm , which is the diameter of silica nanoparticles. Additionally it can be observed that the separation from layer-to-layer on bilayer structured particles, is higher than that observed in the natural clay. This distance

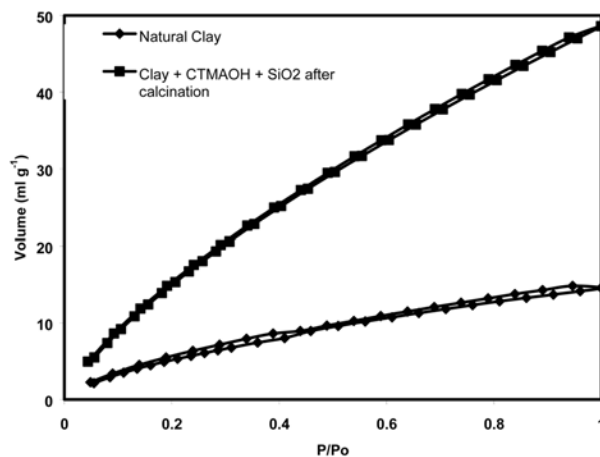


Fig. 6. Hydrogen adsorption isotherms of untreated and SiO_2 intercalated clay.

is around 3.8 nm, and according to Bragg's Law, if a high percentage of material were organized with that separation, the expected 2θ angle must be 2.35° which is not observed in Fig. 4, suggesting thus that distance from layer-to-layer in most cases is at least higher than 3.8 nm.

Figure 6 shows the isotherm of hydrogen adsorption taken at 77 K. Untreated clay presented an hydrogen adsorption capacity of 0.12% w/w, and for intercalated clay the adsorption was 0.4% w/w. As can be seen in Fig. 6, for untreated clay the adsorbed amount of hydrogen at the higher pressure is only 2.5 times that obtained at the beginning of isotherm, indicating thus that there is no availability of mesoporous. Nevertheless, for the intercalated clay the adsorption changes from 4 ml g^{-1} for $P/P_0 = 0.05$ to more than 40 ml g^{-1} for the highest pressure, which implies that the main contribution of the hydrogen storage comes from the mesoporosity developed. Since the ratio of hydrogen adsorption capacity/surface area in both cases is around 4, probably the adsorption capacity is restricted to a hydrogen monolayer by the nature of the surface, and multilayer adsorption does not occur during storage capacity measurements in the conditions studied.

As a future study adsorption capacity must be determined at higher pressures in order to know whether multilayer adsorption can be carried out on the high pore volume created by the assembly of the clay/silica nanostructure. Another possibility is the tailoring of the exposed surface to a more hydrogen-compatible nature, in order to increase the compatibility of surfaces with hydrogen.

Conclusions

Natural montmorillonite clay was intercalated with silica nanoparticles and almost a total delamination of clay was obtained, thus allowing the availability of each side

of the clay layers for gas adsorption. According to TEM images and XRD patterns, the layers of clay are separated in such a way that diffusion of molecules to the interlayer is not restricted by the walls of the channels, since the separation between layers is at least 3.8 nm and in many cases the separation is given by the diameter of SiO_2 nanoparticles, which is around 12 nm. Hydrogen adsorption increased from 0.12 to 0.40% w/w which is directly proportional to the surface area increase. Future work is proposed to take benefit of the surface area and pore volume generated by the assembling of almost single clay layers intercalated with SiO_2 nanoparticles.

Acknowledgements

This study was supported by CONACYT (Grant No. 47776).

References

1. S.Ch. Hsieh and Chih-Ju G. Jou, *Appl. Thermal Engineering* 27 (2007) 2924-2928.
2. W.C. Lattin and V.P. Utgikar, *Int. J. of Hydrogen Energy*, 32[15] (2007) 3230-3237.
3. L.L. Vasiliev, L.E. Kanonchik, A.G. Kulakov and V.A. Babenko, *Int. J. of Thermal Sciences* 46 (2007) 914-925.
4. M. Hirscher and B. Panella, *Journal of Alloys and Compounds* 404-406 (2005) 399-401.
5. M.Z. Figueroa-Torres, A. Robau-Sánchez, L. De la Torre-Saénz and A. Aguilar-Elguézabal, *Microporous and Mesoporous Materials* 98 (2007) 89-93.
6. Y.Y. Fan, A. Kaufmann, A. Mukasyan and A. Varma, *Carbon*, 44[11] (2006) 2160-2170.
7. G.R. Armando, Luis de la Torre, L.A. García-Serrano and A. Aguilar-Elguézaba, *J of Colloid and Interface Science*, 274[2] (2004) 550-554.
8. S. Kawi, *Materials Letters* 38 (1999) 351-355.